Scientific Research and Essays Vol. 7(7), pp. 751-773, 23 February, 2012
Available online at http://www.academicjournals.org/SRE
DOI: 10.5897/SRE10.748
ISSN 1992-2248 ©2012 Academic Journals

Full Length Research Paper

A comparative study on conventional push-over analysis method and incremental dynamic analysis (IDA) approach

Navideh Mahdavi[1]*, Hamid Reza Ahmadi[2] and Hamed Mahdavi[3]

[1]Faculty of Engineering, Marand Branch, Islamic Azad University, Marand, Iran.
[2]Faculty of Civil and Environmental Engineering, Tarbiat Modares University, Tehran, Iran.
[3]Faculty of Civil and Environmental Engineering, Tabriz University, Tabriz, Iran.

Accepted 22 August, 2011

The main objective of this paper is to evaluate the load-displacement capacity of steel moment-resisting frame structures using the conventional non-linear static analysis method and incremental dynamic analysis approach. Emphasis was put on the influence of different lateral load patterns on the plastic hinge of structural components and also on the seismic behavior of the structures which is influenced by the behavior of their components [(EEsof, electronic engineering software)]. Firstly, to get an idea, two simple frames were selected and analytically tested using the conventional push-over and then the results were compared with dynamic analysis approach using a simple harmonic time-history. The results show that the axial forces in columns obtained from dynamic approach are smaller than those of the other non-linear static methods and this influences the plastic hinge lengths. Then three sets of steel moment-resisting frames were loaded under different load patterns frequently used in conventional push-over analysis methods. The outputs of the structural analysis, in the forms of story shear versus story drift ratios of upper, middle and lower portions show that in general, nonlinear static analysis results in smaller axial forces in columns which cause smaller component deformations, thus weaker structural load-deformation capacities.

Key words: Performance- based engineering, nonlinear static analysis, lateral load pattern, plastic hinge.

INTRODUCTION

The simplicity of push-over analysis approach and its capability in providing structural nonlinear response information served well as an alternative to time-history analysis method. This method can be employed to identify the seismic resisting components in which inelastic deformations are expected to be high or might cause important changes in inelastic dynamic structural response characteristics (Krawinkler and Seneviratna, 1998). Moreover, this type of analysis provides more realistic estimation of force-demand of brittle components, and thus verifying the adequacy of structural safety in tolerating destructive strong motion. One of the main objectives of this paper is to demonstrate that the non-linear static (pushover) analysis approaches prescribed in FEMA 273 (1997) and FEMA 356 (2000) produce completely different plastic hinge lengths for the columns of selected structures and therefore result in different capacity curves. And also, it will be shown that the deviation of capacity curves using FEMAs provisions and time-history analysis is a good evidence for the weakness of this procedure.

Nonlinear static analysis

Nonlinear static analysis (push-over) method (NSAM) is an approximate analysis method through which an increasing lateral load with an invariant high-wise

*Corresponding author. E-mail: NVDH_Mahdavi@marandiau.ac.ir. Tel: (+98) 09144100860. Fax: (+98411) 5561088.

distribution is applied to a mathematical model of structure until a target displacement is reached and/or the structure collapses. In this analysis method, lateral load pattern represents the likely distribution of inertia forces imposed over the height of structure during an earthquake. The distribution of inertia forces vary with the severity of the earthquake and time throughout its duration. However, in traditional pushover analysis approaches, generally, an invariant lateral load pattern is used. Generally speaking, two different non-linear static analysis approaches (push-over) are found in literature (Antoniou and Pinho, 2004a; Antoniou and Pinho, 2004b; Papanikolaou et al., 2005).

i) Constantly fixed applied load increment.
ii) Instantaneously updated applied load increment.

The first family of non-linear static method consists of non-adaptive analysis approaches which are based on incremental lateral load in the forms of triangular, uniform and those compatible with the first mode shape pattern. Conventional push over approach is an example of this family (ATC-40, 1996; FEMA 273, 1997; FEMA 356, 2000). The second family of static non-linear analysis (push-over) method is those in which the applied load is constantly updated depending on the instantaneous dynamic characteristics of the structure. Adaptive first mode pushover method and adaptive full modes are samples of this family.

Conventional push-over analysis

Conventional push-over analysis, commonly used for the assessment of building structures is a nonlinear-iterative solution of the well-known static equilibrium equation KU = P, where K is the nonlinear stiffness matrix (tangent stiffness), U is the displacement vector and P is a predefined load vector applied laterally over the height of the structure in a small load increment forms. This lateral load is a fixed pattern with constant ratio throughout the analysis procedure. In such methods, inelastic static is traced to the single degree of freedom system (derived by Gulkan and Sozen (1974) to represent the multi-degree of freedom via an equivalent structure). Saiidi and Sozen (1981) and Fajfar and Fischinger (1988) proposed a simplified inelastic analyses approach for multi-degree of freedom systems to represent the multi-degree of freedom via an equivalent structure. The main point in the use of equivalent system of Equation 1 (Naeim, 2001) is that, since the response of system decreases as the damping ratio is increased, the nonlinear response of the system is related mathematically (and not physically) to the damping ratio in the following form:

$$\ddot{\chi}_{eq} + 2\xi_{eq}\omega_{eq}\dot{\chi}_{eq} + \omega_{eq}^2\chi_{eq} = -\ddot{\chi}_g \quad (1)$$

Where ξ_{eq} and ω_{eq} are the viscous damping ratio and natural circular frequency of the equivalent linear system respectively. For a bilinear system, the time period T_{eq} of the equivalent system as compared to T_0 of the original system is given by:

$$T_{eq} = T_0\sqrt{\frac{\mu}{(1-\alpha)+\alpha\mu}} \quad (2)$$

Where μ is the ductility coefficient, and α is the ratio of the positive post-yield stiffness to the original stiffness. The equivalent damping is given by:

$$\xi_{eq} = \xi_0 + \frac{2}{\pi}\left[\frac{(1-\alpha)(\mu-1)}{\mu-\alpha\mu+\alpha\mu^2}\right] \quad (3)$$

ξ_{eq} in Equation 1 is introduced in the following form (ATC-40 1996):

$$\xi_{eq} = \xi_0 + \chi\xi_h \quad (4)$$

In Equation 4, ξ_{eq} is limited to 45%, χ is equal to 1.0 for ξ_h = 16.25% and 0.77 for ξ_h = 45% with linear interpolation for other damping values.

The aforementioned procedure continues until a predefined limit state such as immediate occupancy, life safety or collapse prevention is reached or until structural collapse is detected. The push-over analysis may be performed using force-control or displacement-control approach. In the former fashion, the structure is subjected to an incremental lateral load pattern and corresponding displacements are calculated while in the latter, the structure is subjected to a deformation profile and lateral forces necessary to generate such displacements are computed. The first option is commonly preferred since the displacement is not known. FEMA 356 (2000) requires the push-over plot to be performed by applying monotonically increasing lateral force vectors with a constant vertical profile in the forms of triangular or uniform distribution. ATC-40 (1996) suggests the capacity spectrum method (CSM) and will be discussed in the next study.

Incremental dynamic analysis approach (IDA)

Several methods are being proposed to tackle the problem of accurate estimation of the seismic demand and capacity of structures. One of the promising candidates is IDA (Vamvatsikos and Cornell, 2005; FEMA440, 2005). IDA is a procedure that offers demand and capacity prediction capability in regions ranging from elasticity to global dynamic instability by using a series of

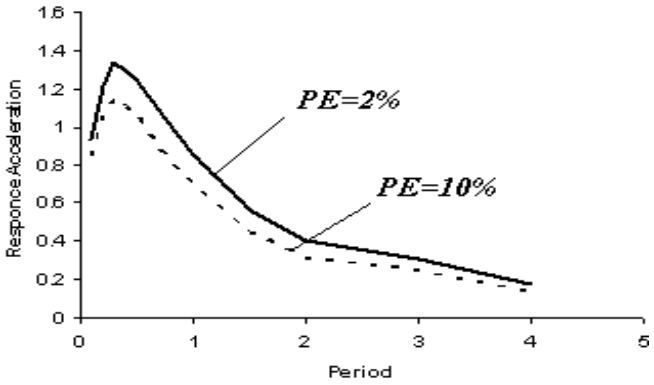

Figure 1. Estimated response spectra for the selected site.

non-linear dynamic analyzing under suitably multiply-scaled ground motion records. This approach needs time-histories to be scaled and applied to the structure. For this purpose, the uniform response spectra, corresponding to the probability of exceedence, PE = 10 and 2%, of the selected region were estimated through a site specific hazard analysis using the well known PSHA method. Probabilistic seismic hazard analysis (PSHA) was performed on the basis of Cornell-McGuire method and the uniform hazard spectra corresponding to the probability of exceedence 10 and 2%, (PE = 10 and 2%) of the site were estimated. According to Cornell (1968, 1971) and McGuire (1995, 2004), modern PSHA is based on the following equation:

$$\gamma(y) = \sum \upsilon p[Y \geq y] = \sum \upsilon \int\int \left\{ 1 - \int_0^y \frac{1}{\sqrt{2\pi}\delta_{\ln,y}} \exp \left[-\frac{(\ln y - \ln y_{mr})^2}{2\delta_{\ln,y}^2} \right] d(\ln y) \right\} f_m(m)\, f_R(r) dm dr \quad (5)$$

Where *v* is the activity rate, *fM* (*m*) and *fR* (*r*) are the probability density function (PDF) of earthquake magnitude (*M),* and *R* epicenteral or focal distance respectively. *ymr* and *σln*, *y* are the median and standard deviation at *m* and *r*. *fM* (*m*) and *fR* (*r*) were introduced to account for the variability of earthquake magnitude in the selected region and the corresponding epicenteral or focal distance respectively. (Campbell, 1981; Joyner and Boore, 1981; Abrahamson and Silva, 1997; Toro and others, 1997; Atkinson and Boore, 2006; Akkar and Bommer, 2007).

The well known computer program SEISRISK III (Bender and Perkins, 1987) was used for hazard analysis procedure. A collection of available earthquakes consisting the recorded and historical events was used for calculating the b value for the selected region based on Gutenberg-Richter relation (b = 0.52). The maximum magnitude value was determined using the well known Kijko (Kijko et al., 1992) approach. The aftershocks were removed using windowing procedure proposed by Gardner and Knopoff (1974). The response spectral-based attenuation relationships proposed by Ambraseys and Simpson (1996), Youngs et al. (1997), Abrahamson and Silva (1997) and Sadigh et al. (1997) with the weights of 0.3, 0.2, 0.2 and 0.3 respectively were incorporated in the model. The peak ground accelerations (PGA) and the elastic response spectra with 5% damping ratio corresponding to the probability of exceedenses 2 and 10% were estimated to be used in performance assessment of the selected structures. The time-histories compatible with the estimated uniform response spectra were determined. Figures 1, 2 and 3 present the estimated response spectra and corresponding compatible time-histories.

METHODOLOGY

Basic concept of push-over analysis

In general, dynamic equilibrium equation of the system is:

$$M\ddot{u}(t) + C\dot{u}(t) + Ku(t) = -M\ddot{u}_g(t) \quad (6)$$

Where, M, C and K are mass, damping and stiffness matrixes, respectively. Equation 6 is solved statically in traditional push-over approaches using the following methods:

a) Equivalent lateral force (ELF).
b) First mode lateral load distribution (SDOF).
c) Multimode lateral load distribution (MDOF).

These types of equation solutions suffer from three basic problems: firstly, modal combination rules SRSS/CQC; secondly, neglecting the time in time-dependent parameters; and thirdly, phase angles of structural dynamic responses. Consequently, the structural responses obtained from these methods, particularly in non-linear behavior, end with the deviation of static results from those of dynamic ones. However, the dynamic solution of the problem can

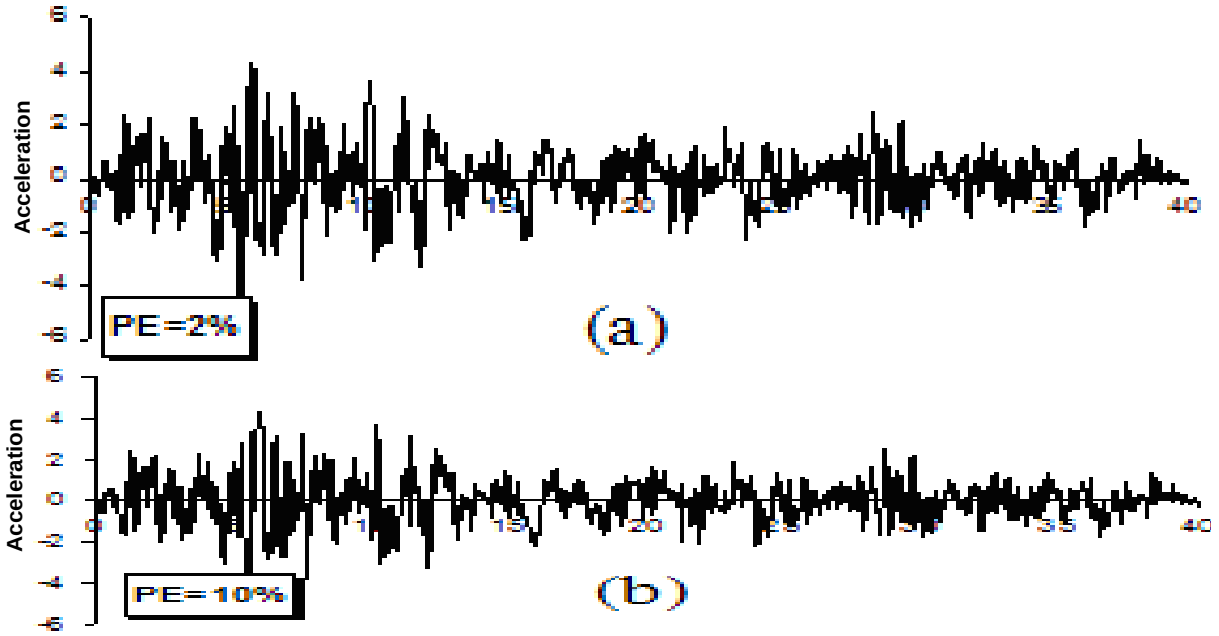

Figure 2. Compatible time-histories corresponding to the estimated response spectra with probability of exceedance: a) 2% and b) 10%.

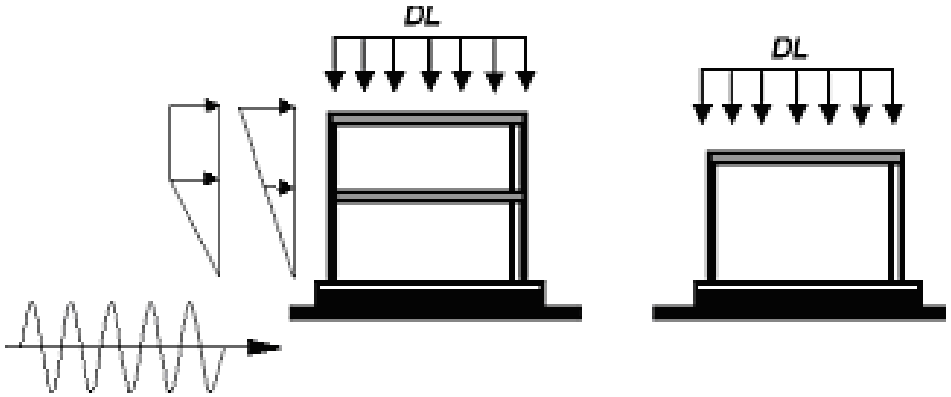

Figure 3. Selected steel moment resisting frames (MRF).

be performed using three, five, or seven acceleration time-histories consistent with the fault rupture, earthquake magnitude, site soil conditions and compatible with the response spectra (ASCE-7, 2005). It is worth mentioning that achieving non-linear responses of structures comparable with those of ASCE-7 (2005) is not the goal of this paper, rather, a comparative study for evaluating the deviation of static solution results from those of dynamic time-history analysis is conducted. Consequently, the time-histories compatible with the estimated specific site response spectra were determined for dynamic time-history analysis of the selected structures.

In other words, it is not claimed that the non-linear responses of selected structures using the compatible time-histories as a reference comply with those of code provisions; rather, the time-history analysis procedure used in this study is free from lateral load patterns.

Simple examples of the problem

Here, it will be illustrated that different lateral load patterns used in conventional push-over methods produce different axial force values in columns of structures, and thus result in different plastic hinge lengths. It will be shown that the difference between the plastic hinge lengths in the columns of these frames, produced by different types of conventional static push-over analysis methods and also time-history analysis is the result of statically solving the dynamic equilibrium equation. Physically, plastic length in the components of a structure, as a capacity, must be free from the type of lateral load pattern. For this purpose, the conventional static non-linear (push-over) analysis methods, frequently used in engineering community were exercised on two simple frames. The linear as well as non-linear responses of simple examples will be discussed identifying the reason why the capacity curves in

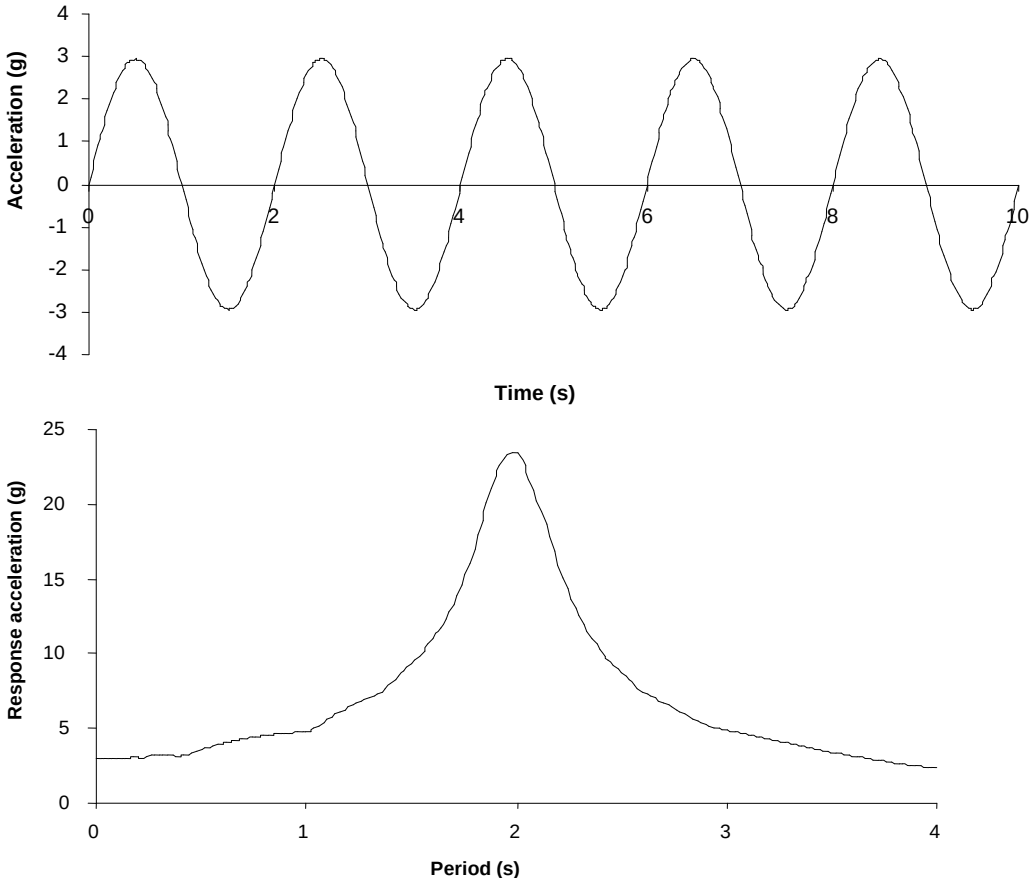

Figure 4. Harmonic load as time history acceleration and corresponding elastic response spectrum.

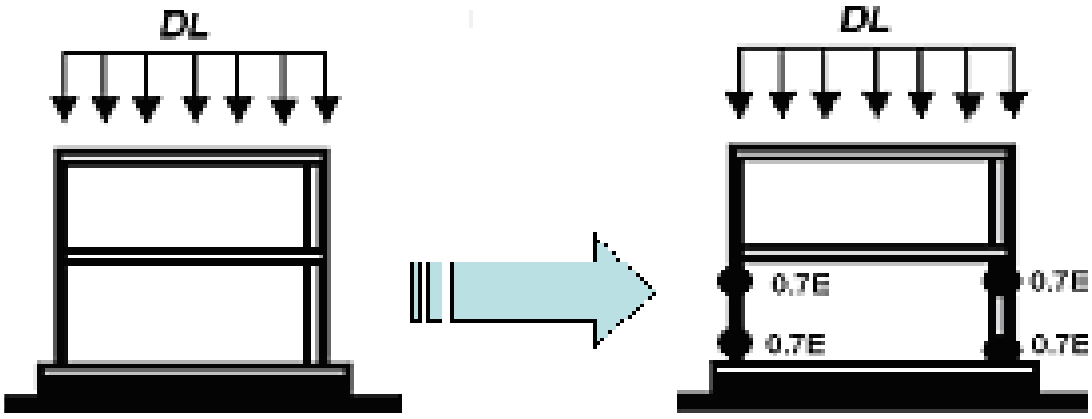

Figure 5. The two story frame with reduced stiffness.

different types of lateral load patterns deviate from those of incremental dynamic analysis approach (IDA) as a comparatively proper reference. Two simple and regular moment resisting frames, a one-storey MRF and a two-storey MRF are designed based on IBC-ASD (International Building Code 2000) under the condition that the first mode natural period of both frames are the same equal to 0.69 s. The selected frames shown in Figure 4 were analyzed linearly and non-linearly due to different lateral load types. A harmonic time history $\ddot{u}_g = 0.3gSin\pi t$ is selected as input lateral force to be used in dynamic method and its response spectra is used in conventional push-over analysis examples. Figure 5 shows the harmonic time history and corresponding acceleration

Table 1a. Frames properties: frames description.

Dead load (kN)	Modulus of elasticity (MPa)	Bay width (m)	Story height (m)	Beams	Columns	Frame description
29.40	2.1e5	5	4	IPE40	Story1 IPB20	
25.48	2.1e5	5	4	IPE40	Story2 IPB18	2-story
25.97	2.1e5	5	6	IPE40	IPB20	1-story

Table 1b. Dynamic characteristics of the selected frames.

Mass participation factor	Frequencies (rad/s)	Period (s)	Dynamic properties
0.891	9.148	1st mode 0.69	2-story
0.109	21.34	0.29 2nd mode	
1	9.148	0.69	1-story

response spectrum respectively.

The natural periods and material properties are also depicted in Table 1. The harmonic acceleration $\ddot{u}_g = 0.3gSin\pi t$ is applied to both frames through two different steps.

Linear static analysis

As the first step, the base shear of both frames V are calculated on the basis of Sa obtained from response spectrum (Figure 5) using Equation 7:

$$V = C1C2C3CmSa.W \quad \text{(FEMA356, 2000)} \tag{7}$$

Where:

V: Pseudo lateral load;
C1: Modification factor to relate expected maximum inelastic displacement to displacement calculated for linear elastic response;
C2: Modification factor to represent the effects of pinched hysteresis shape stiffness degradation and strength deterioration on maximum displacement response;
C3: Modification factor to represent increased displacements due to dynamic p-Δ effects;
Cm: Effective mass factor to account for higher mode mass participation effects;
Sa: Response spectrum acceleration at the fundamental period and damping ratio of the building in the direction under consideration;
W: Effective seismic weight of the building.

Lateral load pattern

Triangular lateral load pattern

The vertical distribution of base shear, V, in this method is given by:

$$F_i = c_{vi}.V \tag{8}$$

$$c_{vi} = \frac{w_i h_i^k}{\sum_{i=1}^{n} w_i h_i^{\,k}} \tag{9}$$

Where,

c_{vx} : Vertical distribution factor;

w_i : Portion of the total building weight W located on or assigned to floor I;

h_i : Height from the base to floor level i.

And k equals to:

$$k = 0.5T + 0.75 \tag{10}$$

Where,

T: the fundamental period of the building in the direction under consideration.

Uniform lateral load pattern

The uniform distribution consisting of lateral forces proportional to the total mass at each level is in the following form:

$$F_i = c_{vi}.V \tag{11}$$

$$c_{vi} = \frac{m_i}{\sum_{i=1}^{n} m_i} \tag{12}$$

First mode lateral load pattern

A vertical distribution proportional to the shape of the fundamental mode in the direction under consideration is in the following fashion:

$$F_i = c_{vi}.V \tag{13}$$

$$c_{vi} = \frac{\phi_i m_i}{\sum_{i=1}^{n} \phi_i m_i} \tag{14}$$

Table 2. Linear responses of simple frames.

MRF	Sa	Pseudo lateral load distribution			Linear static axial force (kgf)	Linear dynamic axial force (kgf)
			Story 2	Story 1		
		Shape	8193	4727		
			6922	5998	11273	
2-story	0.433		8253	4666		
		Triangular	8193	4727		9250
		Uniform	6922	5998	9665	
		First mode	8253	4666	11319	
		srss 1st mode	7353	4157	10469	
		2nd mode	2095	-1022		
1-story	0.433	6239			3605	3610

The axial force in frame columns is calculated using the slope deflection formulation.

Linear dynamic analysis

In the second step, the responses are calculated using dynamic approach. The equilibrium of Equation 6 can be simply reduced to the following form:

$$\ddot{Y}_n + 2\lambda_n \omega_n \dot{Y}_n + \omega_n^2 Y_n = L_n \ddot{g}(t) / M_n^* \quad (15)$$

Where,

M_n^* and L_n are $\{\varphi_n\}^T [M]\{\varphi\}$ and $\{\varphi_n\}^T [M]\{\Gamma\}$.

Equation 15 is solved under a simple support acceleration $\ddot{u}_g = 0.3gSin\pi t$, which gives the response of frames in the form of:

$$Y_i = \frac{L_i}{M_i * w_i} \int_0^t 0.3g * Sin(\pi\tau) * e^{-\zeta w(t-\tau)}$$

$$*Sin(w_D(t-\tau))d\tau \quad (16)$$

Where,

$$u_i = \sum \phi_{in} y_n \quad (17)$$

Table 2 shows the results of the closed form solution in conventional push-over approach using lateral load patterns; triangular, uniform and first mode-based.

Non-linear static analysis step

In the next step, the two-storey frame is non-linearly and dynamically analyzed using the simple harmonic load as ground shaking input time-history. For this purpose, the two first floor column lengths were divided into three elements. The modulus elasticity of elements at the end of columns was reduced to 0.7 of their initial values, thus indicating the lower columns being in non-linear behavior. Figure 6 shows the typical form of reduced stiffness frame. 30% of the primary load was applied to the frame as an incremental static lateral force. As it can be seen in Table 2, the axial force induced in the column of one story frame due to static and dynamic methods are the same while it is different in two- story frame. This point indicates the influence of second mode on the axial forces (Tables 3 and 4). Obviously, the difference is much larger as the structure becomes taller due to the role of different phase between the stories. Again, the two-storey frame was analyzed using different lateral load patterns; triangular, uniform and first mode-based.

Modeling of case studies

In order to assess the capability of conventional pushover method in estimating the nonlinear behavior of structures subjected to seismic loads, three groups of steel moment resisting systems were designed with the span-ratio ranges of H/B<1.5, 1.5<H/B<3 and 3<H/B based on IBC-ASD (2000). The structures were selected with different geometrical characteristics to cover the span ratio from 0.9 to 3.2. Table 6 shows the natural period of the selected structures. Configuration and section properties of the frames are shown in Figures 8 to 10 and Tables 7 to 9, respectively. The material properties are stated in Table 5. The analyses were performed using ZeusNL version 1.7.2 (Elnashai et al., 2010) and the results are shown through four different graphs for each frame.

Plastic hinge

The components of structures undergo large deformations in the post-yield stage while the structure is subjected to strong motion. The deformation takes place at an effective depth along the beams and columns so called “plastic hinge” and is very important in nonlinear analysis procedure. The maximum rotation $\theta_{\max}$ versus maximum bending moment M of the component plastic hinge is chosen as the rotation capacity of beams and also beam-columns under time history/response spectrum ground acceleration. More details on evaluation of post-yield stage, ductility, energy absorption and damage modeling can be found elsewhere (Lakshmanan, 2000, 2003, 2005). Figure 9 presents a typical form of post-yield large deformation (plastic hinge). The dependency of plastic hinge length on the axial column force is discussed here. Parameter "a" which indicates the total elastic-plastic deformation in structural

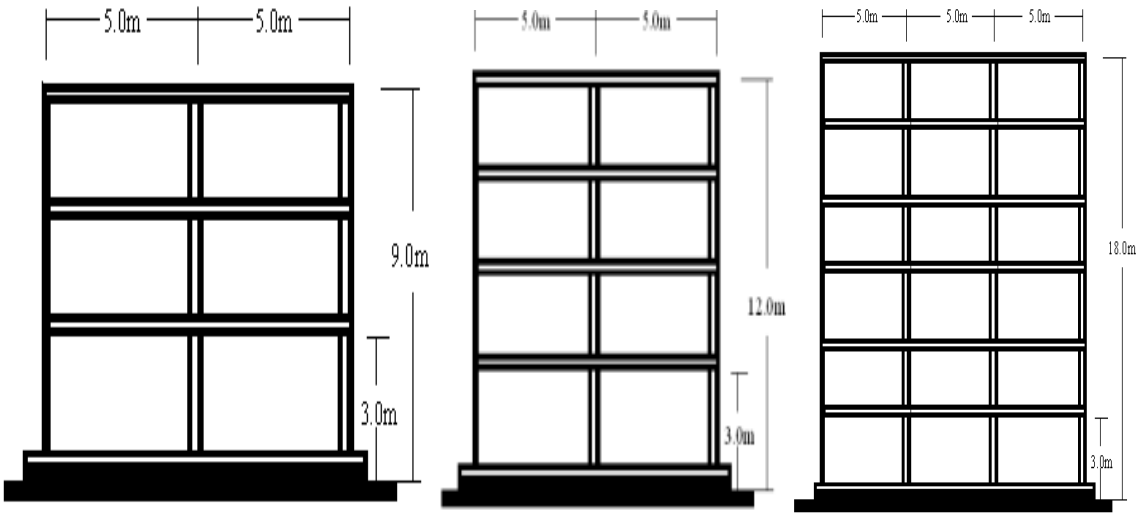

Figure 6. Frames with H/B<1.5.

Table 3. Dynamic characteristic of 2-story frame in non-linear step.

Modal participation factor	Frequencies (rad/s)	Period (s)	Dynamic properties
0.912	8.156	0.77	1st mode
0.088	20.93	0.3	2nd mode

Table 4. Nonlinear static response of axial forces.

Total axial force	Axial force in nonlinear step	Axial force in linear step	Load pattern
16078	4805	11273	Triangular
12695	3030	9665	Uniform
14903	3584	11319	First mode
13134	2665	10469	SRSS
12183	2933	9250	IDA

Table 5. Material properties of selected structures.

Modulus of elasticity	Tensile strength	Yield strength	Material properties
2*10e5 (MPa)	392 (MPa)	235.4 (MPa)	Beams and columns

components depends mainly on: θ_y (FEMA 356, 2000) which itself depends on axial force induced in the members (Equation 18). The more axial force the less θ_y and thus the less "a" value.

$$\theta_y = \frac{ZF_{ye}l}{6EI}(1-\frac{P}{P_{ye}}) \quad (18)$$

Where:

θ_y : Yield rotation,

F_{ye} : Expected yield strength of the material,

I : Moment of inertia,

p : Axial force in member at the target displacement for nonlinear static analyses or at the instant of computation for nonlinear dynamic analyses,

p_{ye} : Expected axial yield force of computation for nonlinear

Table 6. Natural periods of structures.

T4	T3	T2	T1	MRF (story)	Building types
-	0.15	0.23	0.70	3	
0.10	0.15	0.25	0.76	4	H/B<1.5
0.14	0.20	0.36	1.05	6	
0.18	0.27	0.46	1.36	8	
0.19	0.28	0.49	1.48	9	1.5<H/B<3
0.25	0.36	0.36	1.79	12	
0.30	0.42	0.72	1.84	15	H/B≥3
0.32	0.46	0.77	2.09	16	

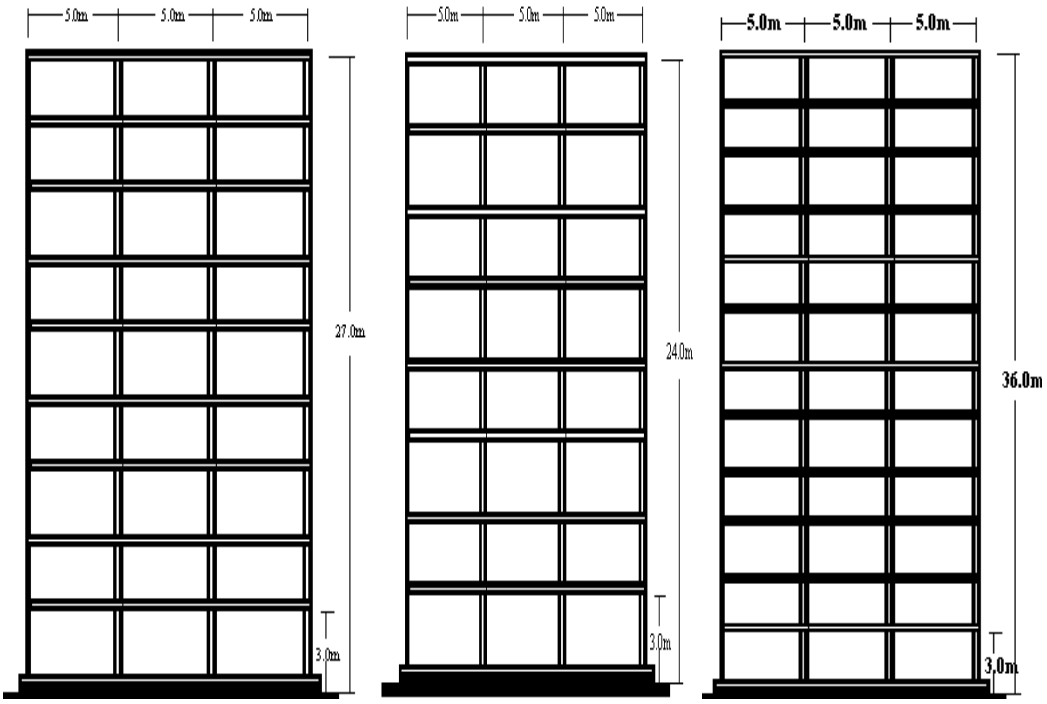

Figure 7. Frames with 1.5 <H/B<3.

dynamic analyses ($A_g F_{ye}$).

Point *A* is the origin; *B* is the point of yielding; *BC* represents the strain-hardening region; *C* is the point corresponding to the maximum force; and *DE* is the post-failure capacity region. The "a" parameter of beam-columns is strongly influenced by the type of structural analysis method. Higher "a" values are obtained in non-linear static-based approaches compared to those of IDA method. Consequently, the non-linear capacity of structures which is directly related to post-yield deformation capacities of components is strongly influenced by the type of load pattern used in non-linear (push-over) analysis approach having considerable deviations from those of time-history analysis. Physically, the capacity of seismic resisting components of structures cannot be dependent on the type of structural analysis (load pattern type), but dependent on the physical strength inherent in the component. Demonstration of this result is the main objective of this study.

RESULTS

Comparing the conventional non-linear (push-over) analysis approaches with those of IDA

Here, the non-linear (push-over) analysis responses of steel MRF structures in three sets of 3, 4, 6, 8, 9, 12, 15 and 16-stories are calculated and compared with those of incremental dynamic analysis method. The uniform response spectrum estimated from a specific site study

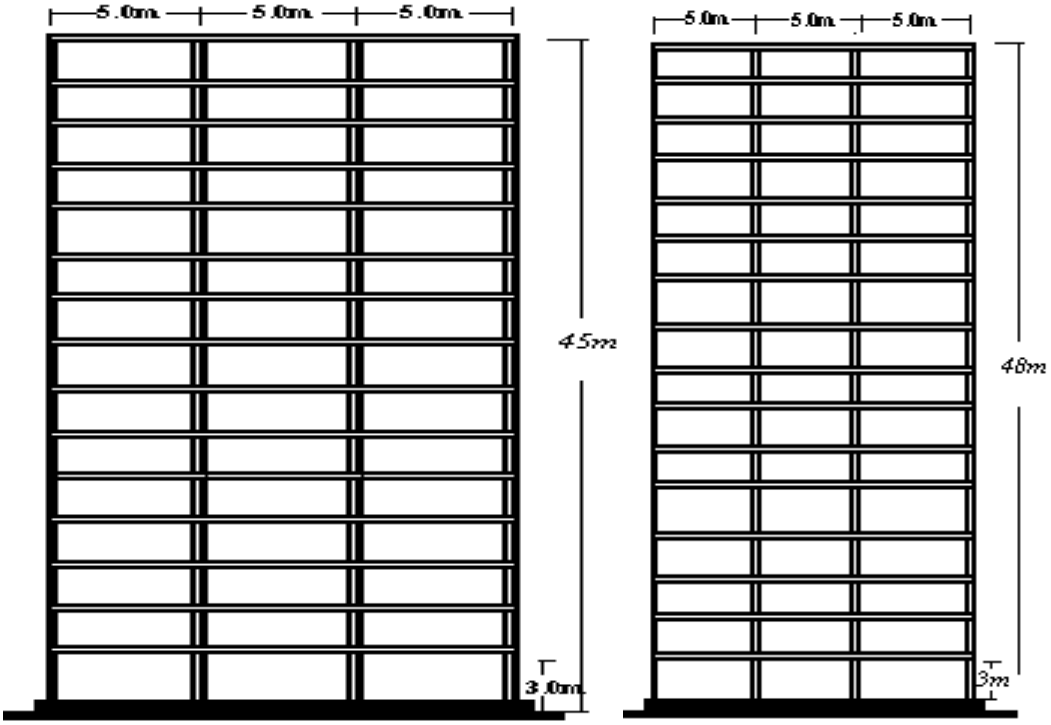

Figure 8. Frames with 3≤H/B.

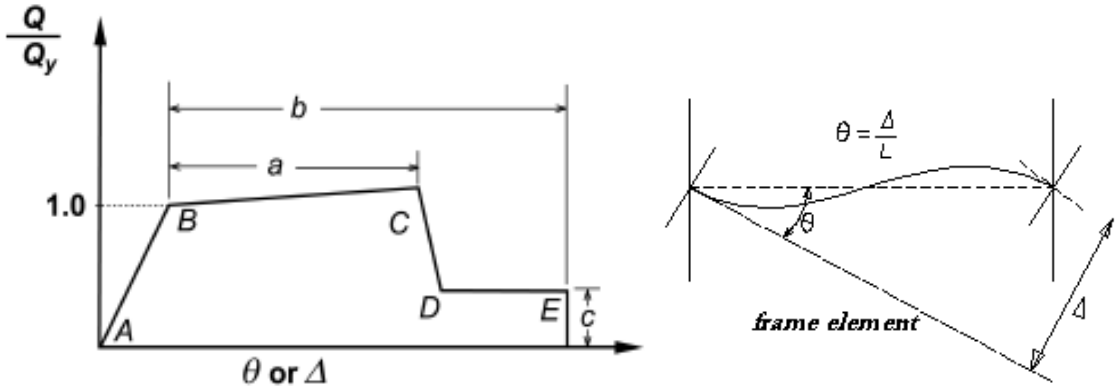

Figure 9. Generalized force-deformation relation.

with probability of exceedance 10% (PE = 10%) was used in static analysis methods while its compatible time-history was used in IDA approach. The comparison of conventional approaches with those of IDA are performed and demonstrated in three steps. Consequently, apart from the usual practice of monitoring base shear versus global drift (so called general level), also, story shear versus interstory drift were included in the evaluation of pushover and IDA analyses. The story shears versus interstory drifts are depicted for three levels of structures, first-storey ratio, middle-storey ratio and top-storey ratio.

The results are shown and discussed in the next study.

Component deformation capacity comparison

Here, the beam and beam-column deformation capacity (plastic hinges) of the selected frames are calculated using the conventional non-linear (push-over) analysis methods and compared with those of IDA approach. Figure 11 and Table 10 show this comparison. It is notable that the capacity curves intended to be strongly method-dependent with a large variation (up to two times) in IDA approach. It means that the uniform load pattern method mathematically demonstrates smaller component deformation capacity and then weaker structural load-

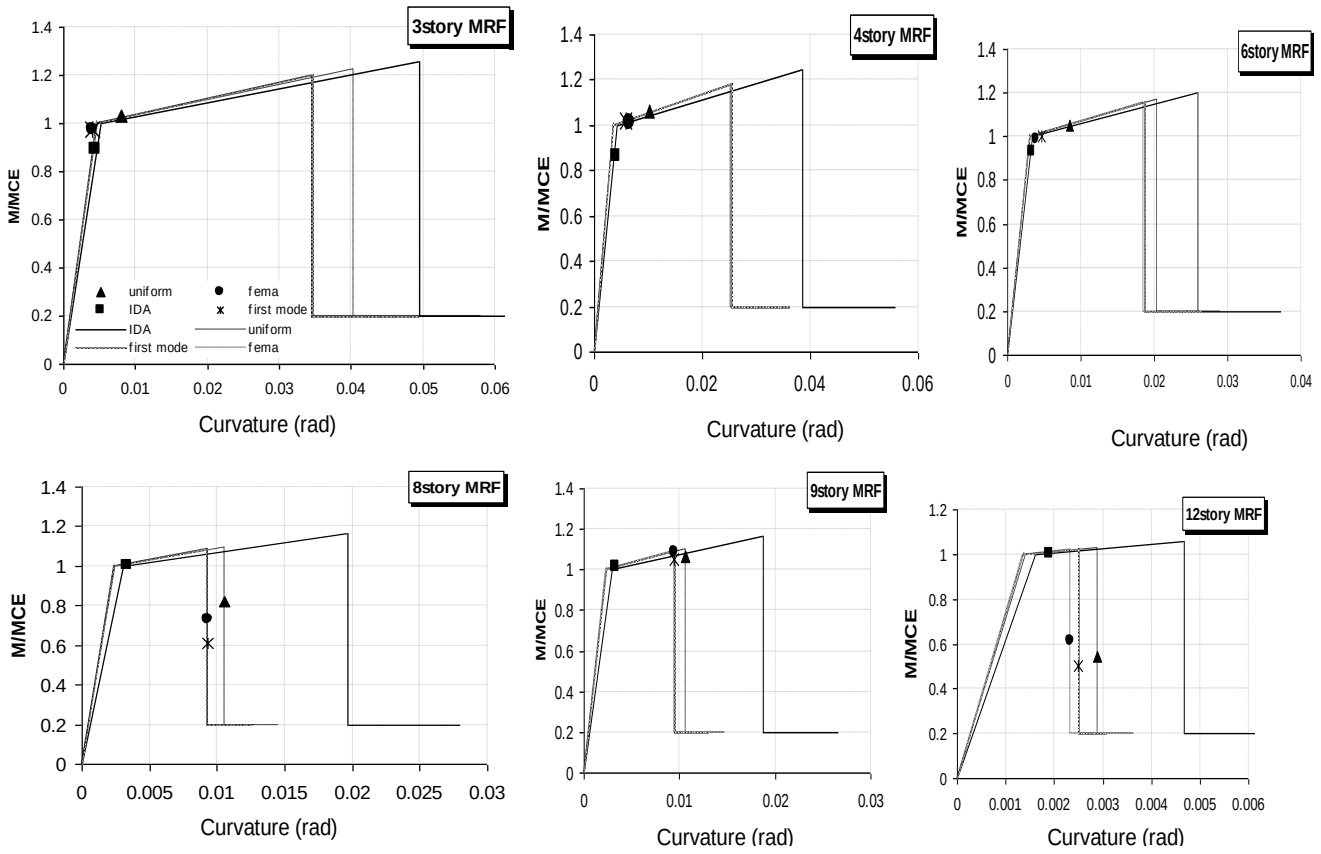

Figure 10. Presentation of the plastic hinge capacity of beam-columns in different methods and corresponding demands.

Table 7. Section specification of frames with H/B<1.5.

Beams columns	Interior columns	Exterior	
IPB20	IPB20	Story1 IPE40	3-story
IPB20	IPB20	Story2 IPE40	
IPB20	IPB20	Story1 IPE40	4-story
IPB24	IPB24	Story2,3 IPE40	
IPB20	IPB20	Story1,2 IPE40	
IPB24	IPB24	Story3 IPE40	6-story
IPB20	IPB20	Story4 IPE40	

deformation strength. The same results can be drawn for the demands of different non-linear static analysis approaches. Interestingly, while the demand in a method is at the first part of the plastic hinge plots, showing the ability of capacity curve (in 8 and 12-story frames); in another method drops from the end, showing somehow the failure of component. Physically, the latter result looks meaningless. Or, while the columns in a method behaves as a displacement control member (in 15 and 16-story frames), it behaves as force control in another approach.

Although a compatible time-history obtained from estimated response spectrum is used in this study, it is not claimed that the results of this study is quantitatively correct; however, sufficient time-histories compatible with source mechanism and path is required for non-linear capacity evaluation of structures. Meanwhile, the technique used in this paper is appropriate for a comparative evaluation of conventional nonlinear (push-over) analysis methods; particularly for assessing the deformability of components.

Table 8. Section specification of frames with1.5<H/B<3.

Beams	Exterior columns	Interior columns	
IPB32	IPB32	Story1,2,3 IPE40	
IPB28	IPB28	Story4,5,6 IPE40	8-story
IPB24	IPB24	Story7,8 IPE40	
IPB34	IPB34	Story1,2,3 IPE40	
IPB30	IPB30	Story4,5,6 IPE40	9-story
IPB28	IPB28	Story7,8,9 IPE40	
IPB40	IPB40	Story1,2,3 IPE45	
IPB36	IPB36	Story4,5,6 IPE45	
IPB32	IPB32	Story7 IPE45	12-story
IPB32	IPB32	Story8,9 IPE40	
IPB28	IPB28	Story10,11,12 IPE40	

Table 9. Section specification of frames with 3≤H/B.

Interior	E×terior	Beams	
Pl35×40×3	Pl35×40×3	Story1 IPE45	
Pl35×35×3	Pl35×35×3	Story2,3 IPE45	
Pl30×30×3	Pl35×35×3	Story4,5 IPE45	
Pl35×35×3	Pl30×30×2.5	Story6,7 IPE45	
Pl30×30×2.5	Pl30×30×2.5	Story8 IPE40	15-story
Pl30×30×2.5	Pl25×25×2.5	Story9,10 IPE40	
Pl25×25×2.5	Pl25×25×1.5	Story11,12 IPE40	
Pl25×25×1.5	Pl25×25×1.5	Story13 IPE40	
Pl25×25×1.5	Pl20×20×1.5	Story14 IPE40	
Pl20×20×1.5	Pl20×20×1.5	Story15 IPE40	
IPB50	IPB50	Story1,2,3 IPE55	
IPB45	IPB45	Story4 IPE55	
IPB45	IPB45	Story5,6,7 IPE50	
IPB36	IPB36	Story8,9,10,11 IPE45	16-story
IPB28	IPB28	Story12 IPE45	
IPB28	IPB28	Story13,14 IPE40	
IPB24	IPB24	Story15,16 IPE40	

Moreover, the similarity of beam capacity curves is shown in Figure 12. Clearly, the independency of beams of axial force is the best reason for the same capacities.

Comparison of force-displacements

Capacity curve (base shear versus roof displacement) represents the global non-linear response of structures subjected to strong motions. To make a comparison between the capacity curves (push-over) obtained from the aforementioned three load patterns and those of IDA approach, three sets of steel structures 3, 4, 6, 8, 9, 12, 15 and 16-stories were designed and the nonlinear static (push-over) analyses of the designed structures were performed using the aforementioned methods. The storey shears versus storey drift ratios of upper, lower, and middle stories were depicted for comparison purpose and demonstrating their response differences with those of non-linear IDA approach (Figures 13 to 23). The comparison process was extended to the second performance indicator, the story shear versus interstory drift. The story force was derived by adding all individual element shear forces and three levels were selected:

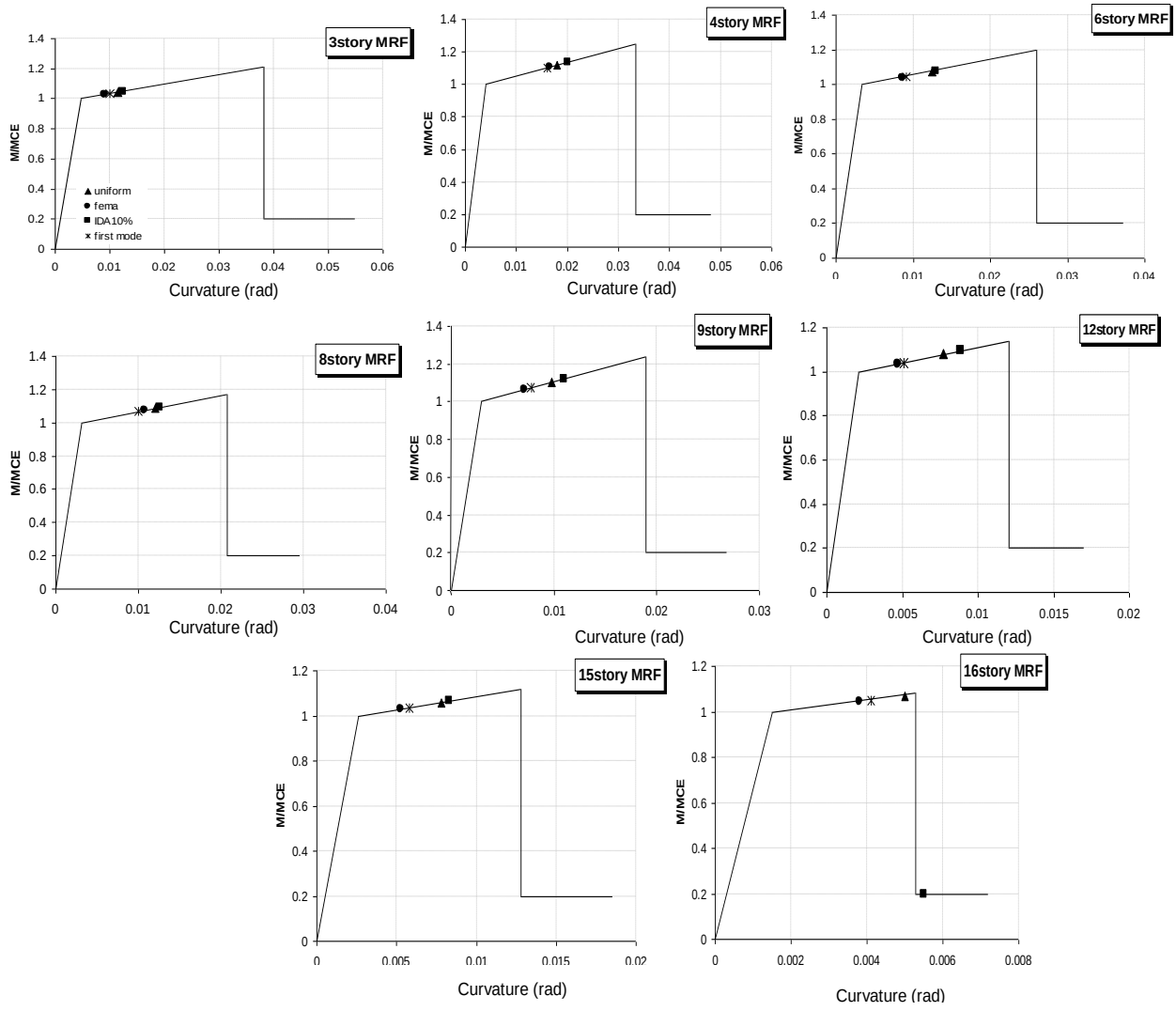

Figure 11. Presentation of the plastic hinge capacity of beams in different methods and corresponding demand.

first, middle and top.

Frames with span-ratio ranges of H/B<1.5

Figure 12 explains the non-linear response comparison of frames in general level; Figure 13 gives non-linear response comparison of frames in first level; Figure 14 gives the non-linear response comparison of frames in middle level; and Figure 15 gives non-linear response comparison of frames in top level.

Frames with span-ratio ranges from 1.5 to 3

Figure 16 explains non-linear response comparison of frames in general level; Figure 17 gives non-linear response comparison of frames in first level; Figure 18 gives non-linear response comparison of frames in middle level; and Figure 19 gives non-linear response comparison of frames in top level.

Frames with span-ratio ranges of H/B≥3

Figure 20 gives non-linear response comparison of frames in general level; Figure 21 explains non-linear response comparison of frames in first level; Figure 22 explains non-linear response comparison of frames in middle level; and Figure 23 explains non-linear response comparison of frames in top level.

Measuring the used pushover techniques accuracies

Since the damage of structures is directly related to local

Table 10. Parameters of columns.

c	b	a	Axial force		Section	
0.2	10.1	6.74	456	Triangular	IPB24	3-story
0.2	10.24	6.83	443	Uniform		
0.2	10.1	6.74	456	First mode		
0.2	12.7	8.50	210	IDA		
0.2	8.96	5.97	704	Triangular	IPB28	4-story
0.2	8.90	5.94	709.9	Uniform		
0.2	8.96	5.97	704	First mode		
0.2	10.9	7.32	468	IDA		
0.2	7.65	5.09	1062	Triangular	IPB32	6-story
0.2	7.64	5.1	1064	Uniform		
0.2	7.63	5.09	1065	First mode		
0.2	9.9	6.62	733	IDA		
0.2	4.25	2.84	1554	Triangular	IPB32	8-story
0.2	4.8	3.20	1475	Uniform		
0.2	4.20	2.80	1562	First mode		
0.2	8.1	5.55	965	IDA		
0.2	4.55	3.03	1590	Triangular	IPB34	9-story
0.2	5.1	3.41	1504	Uniform		
0.2	4.59	3.06	1583	First mode		
0.2	8.1	5.43	1044	IDA		
0.2	5.3	3.55	1922	Triangular	IPB40	12-story
0.2	5.5	3.69	1879	Uniform		
0.2	5.35	3.54	1914	First mode		
0.2	6.6	4.41	1666	IDA		
0.2	-	-	4341	Triangular	PL35x40x3	15-story
0.2	-	-	3841	Uniform		
0.2	-	-	4265	First mode		
0.2	7.1	4.72	2358	IDA		
0.2	-	-	4303	Triangular	IPB50	16-story
0.2	-	-	4140	Uniform		
0.2	-	-	4292	First mode		
0.2	3.9	2.6	2417	IDA		

deformations, the inter-story drifts can be used as comparison criteria for different schemes. The standard error through the whole nonlinear deformation may be defined in the following form (Papanikolaou et al., 2005):

$$Error(\%) = 100\left[\frac{1}{n}\sum_{i=1}^{n}\left|\frac{\Delta_{iD} - \Delta_{iP}}{\Delta_{iD}}\right|\right] \quad (20)$$

Where Δ_{iD} is the inter-storey drift at a given level *i* from the IDA, Δ_{iP} is the corresponding inter-storey drift from the pushover analysis and *n* is the number of the IDA steps.

More accurate response is obtained as the standard error tends to zero.

The standard errors for three lateral load patterns used in conventional push-over approach are calculated and showed in Table 11.

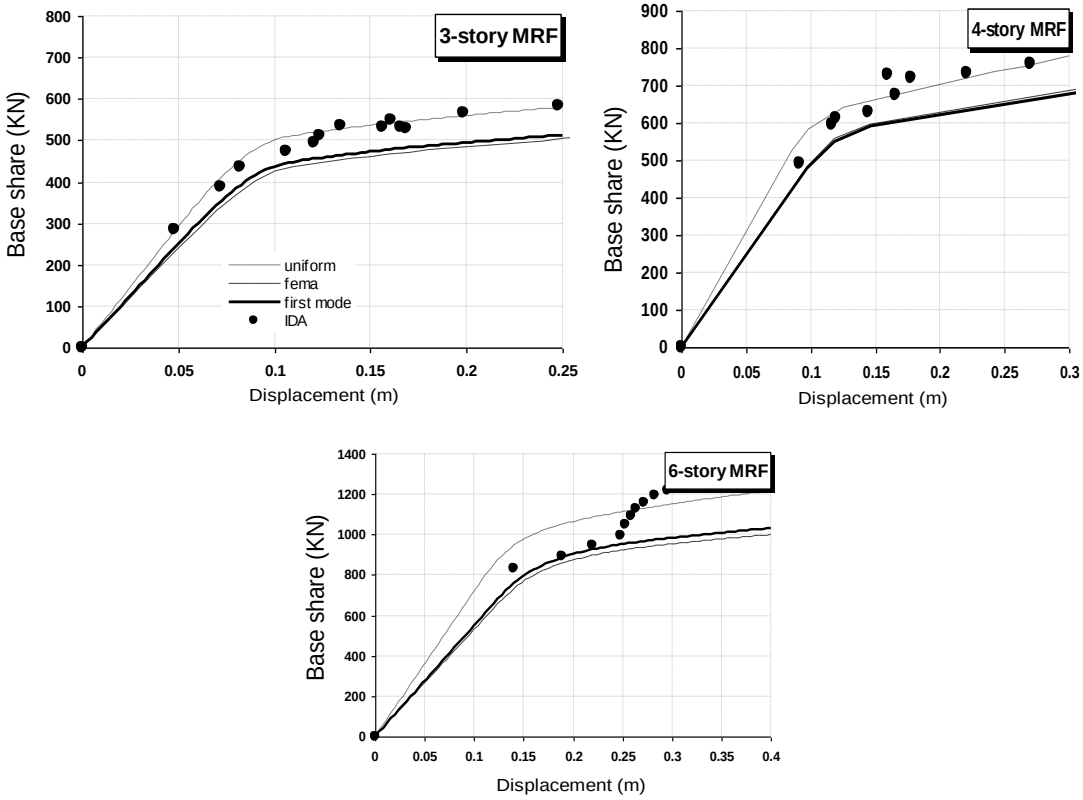

Figure 12. Non-linear response comparison of frames in global level.

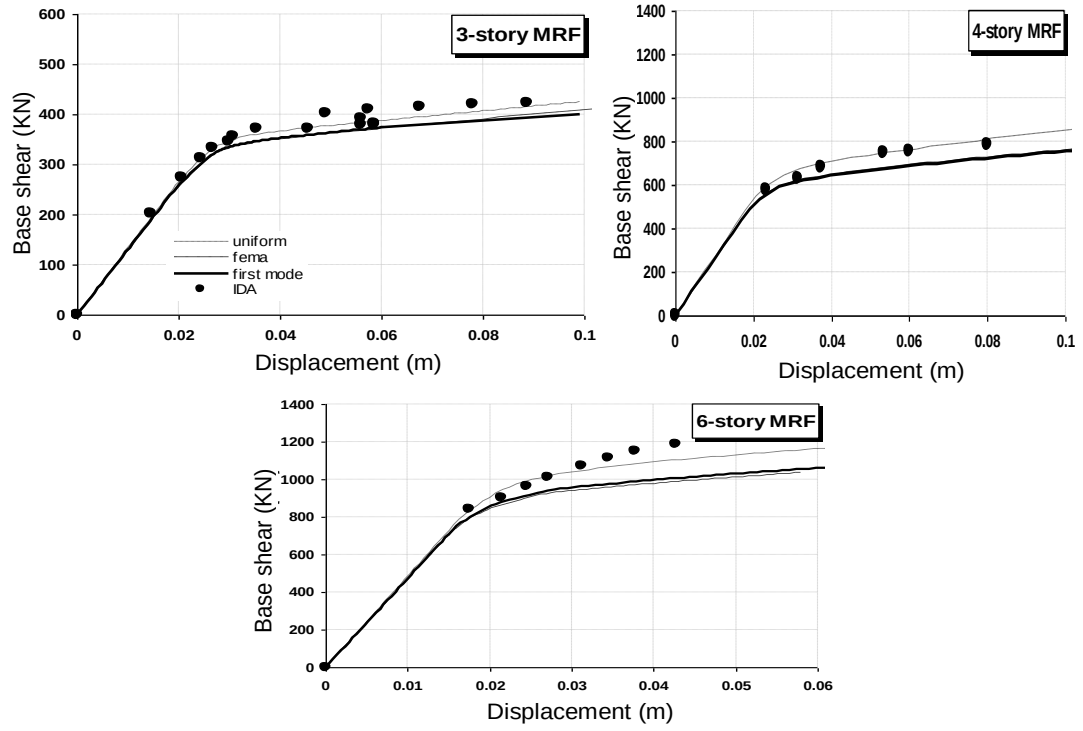

Figure 13. Non-linear response comparison of frames in first level.

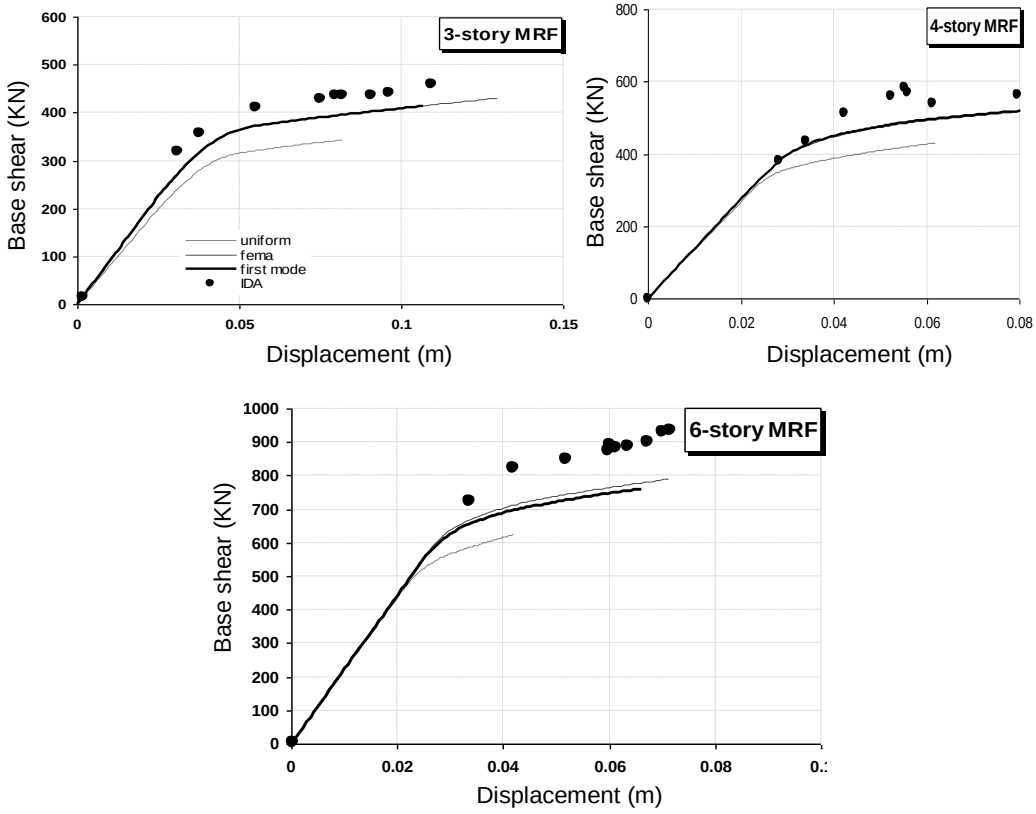

Figure 14. Non-linear response comparison of frames in middle level.

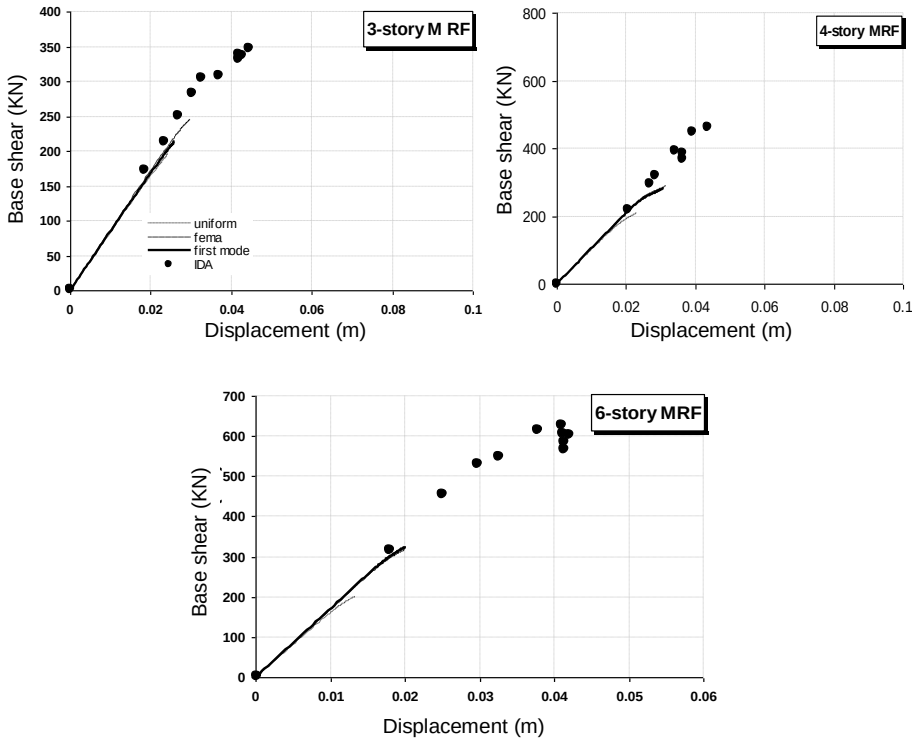

Figure 15. Non-linear response comparison of frames in top level.

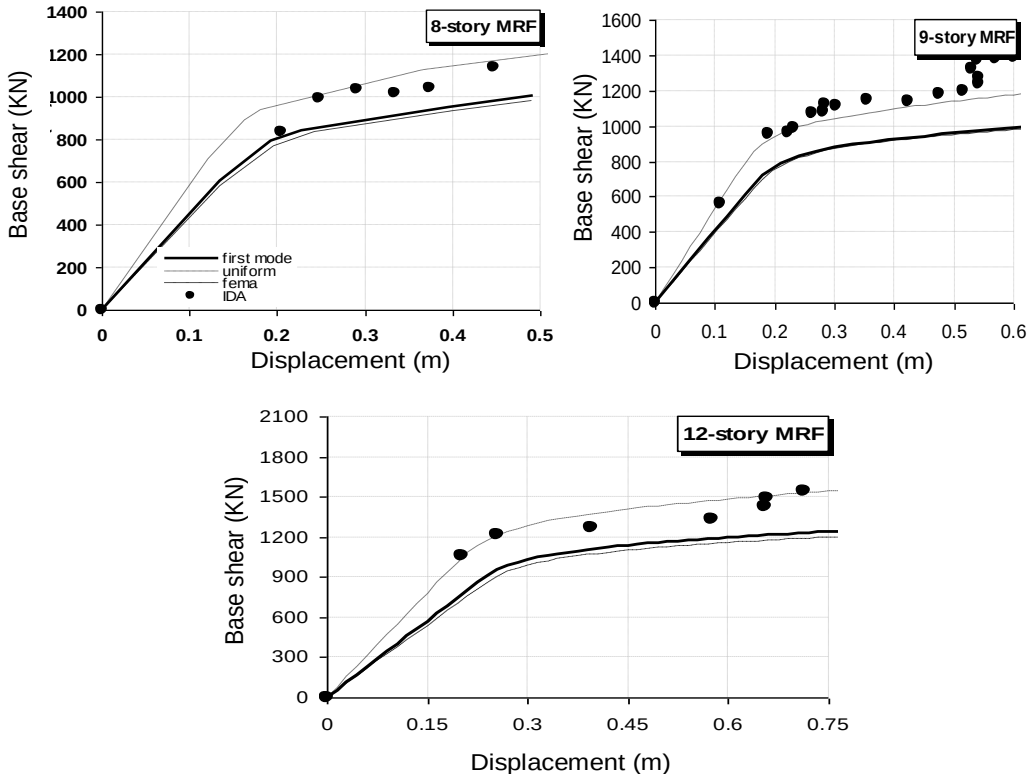

Figure 16. Non-linear response comparison of frames in global level.

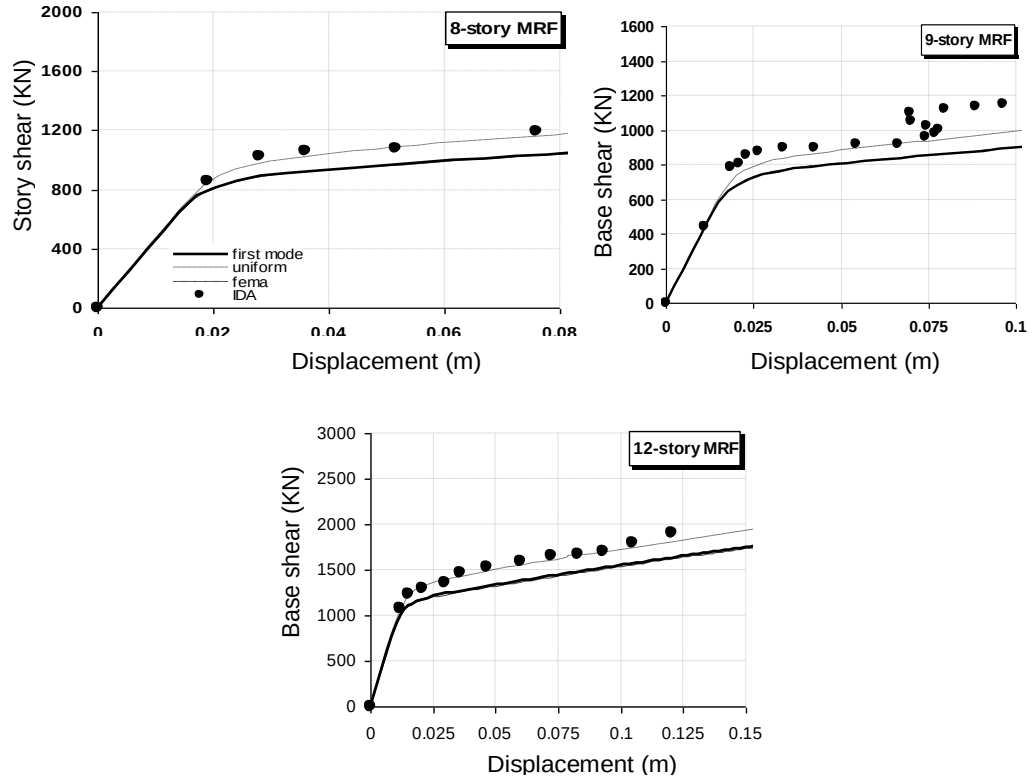

Figure 17. Non-linear response comparison of frames in first level.

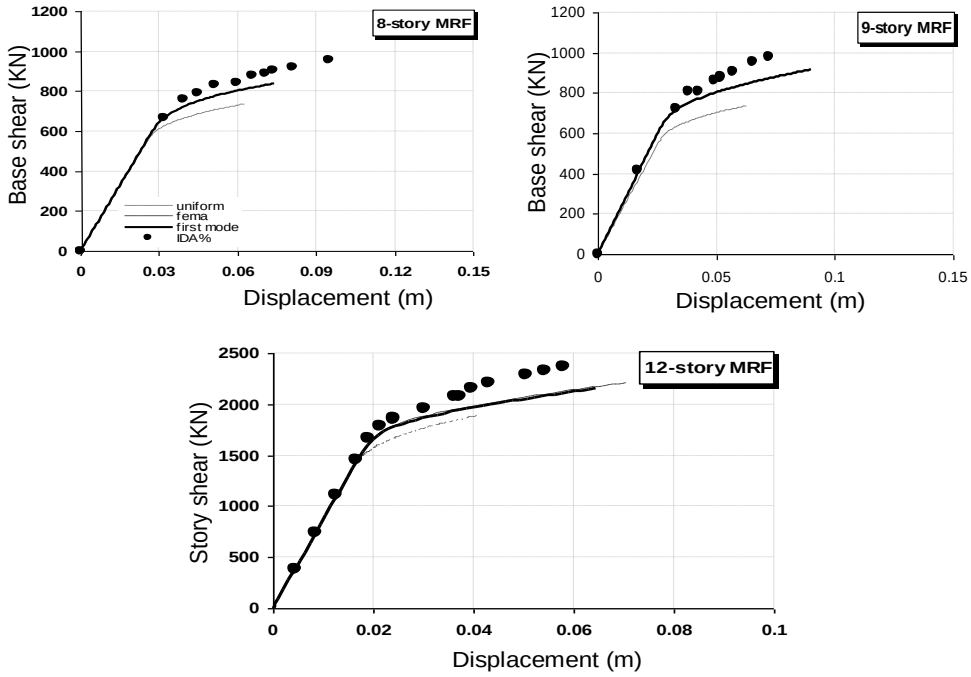

Figure 18. Non-linear response comparison of frames in middle level.

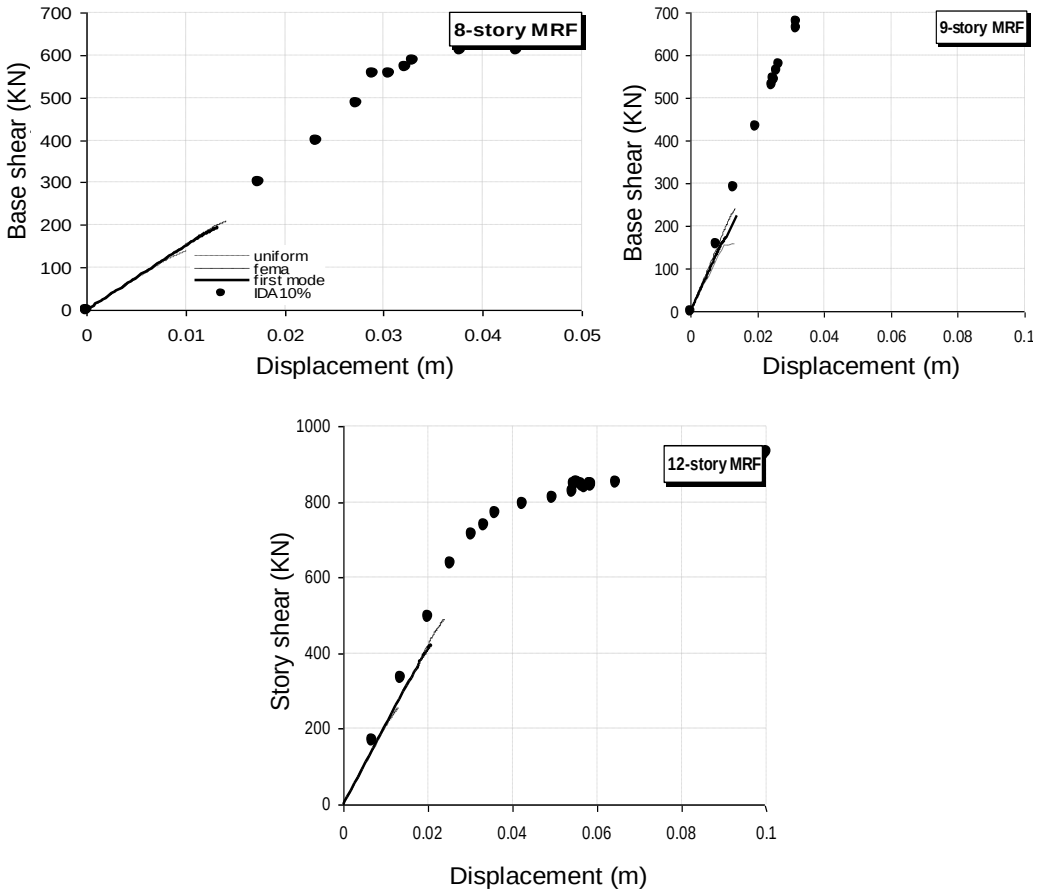

Figure 19. Non-linear response comparison of frames in top level.

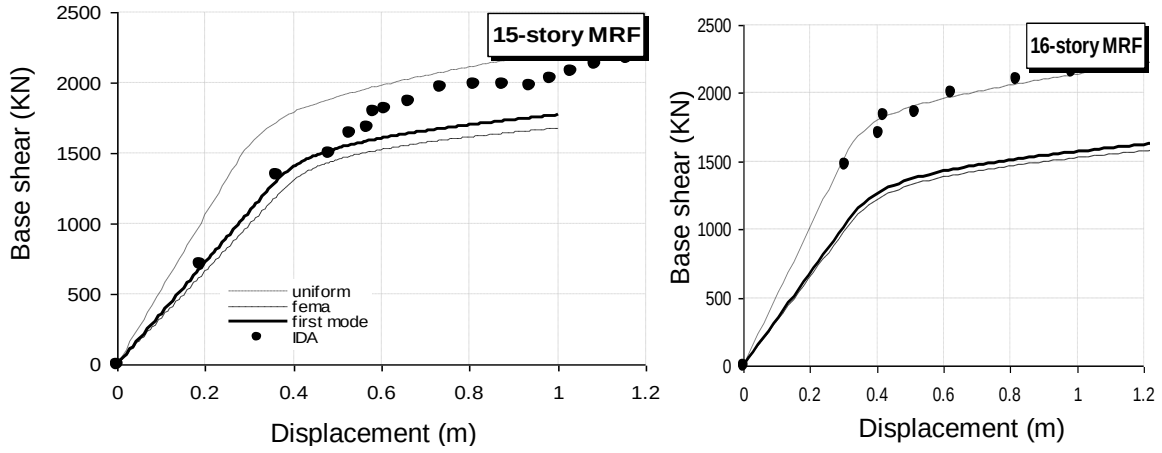

Figure 20. Non-linear response comparison of frames in global level.

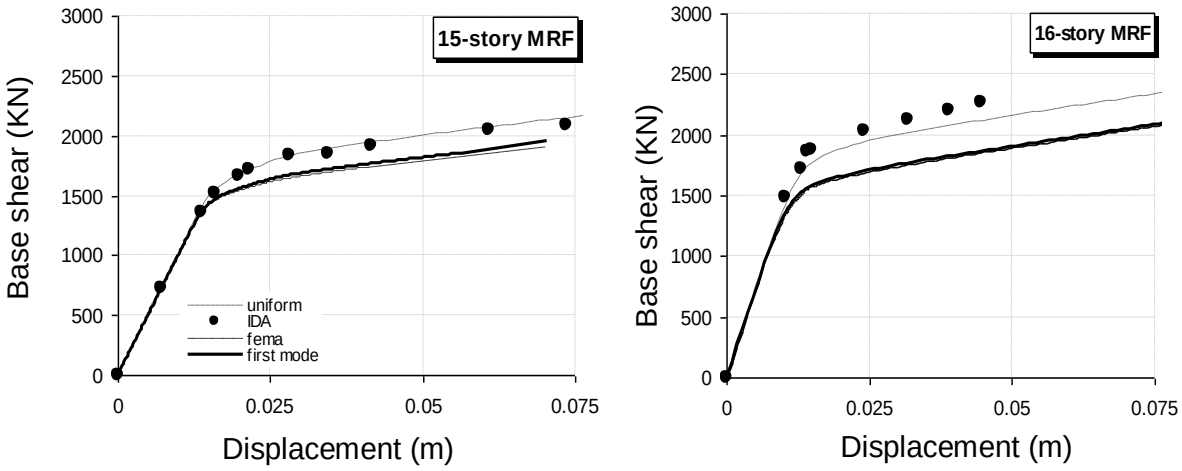

Figure 21. Non-linear response comparison of frames in first level.

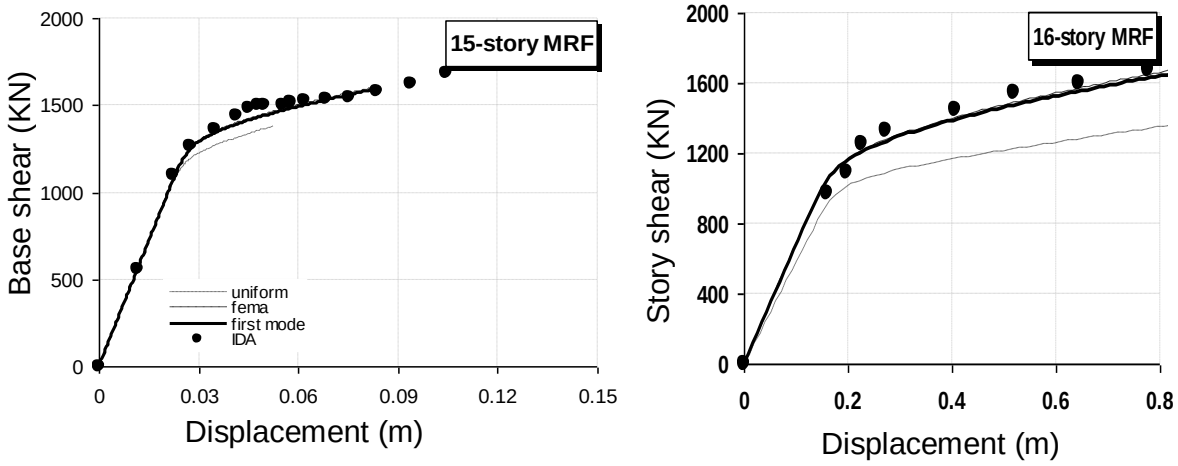

Figure 22. Non-linear response comparison of frames in middle level.

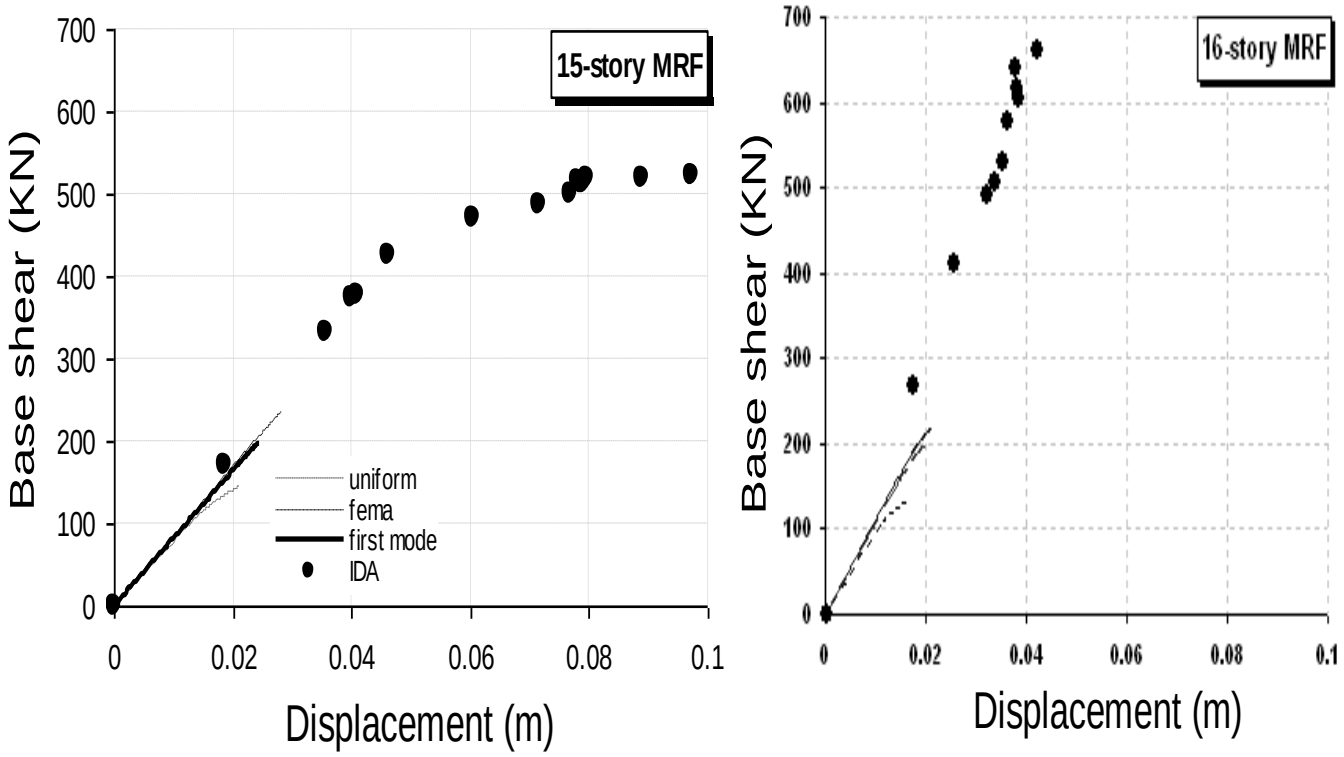

Figure 23. Non-linear response comparison of frames in top level.

Comparison of structural demand points

The inelastic displacement demand referred as target displacement or "performance point" represents the maximum global displacement of structure when exposed to probable earthquake. Here, the performance points obtained from the conventional push-over method (ATC-40, 1996, procedure B) are calculated and compared with those of IDA scheme estimated through a hazard analysis procedure with the probability of exceedance 10% (PE = 10%). The results of such comparison can be seen in Table 12.

DISCUSSION

It includes a discussion on the comparison and evaluation of results obtained from pushover analysis using different approaches. Briefly, this part is summarized in Table 13.

Conclusion

The frequently used static non-linear (push-over) analysis approaches including different types of lateral load patterns; inverted triangular, uniform, first mode-base, full mode and adaptive load patterns were briefly reviewed and their shortcomings/merits were evaluated through two simple examples and three sets of steel frames. The IDA approach based on two levels of probability of exceedance 10 and 2% were presented as promising candidates that offer thorough demand and capacity prediction capability in regions ranging from elasticity to global dynamic instability. In order to highlight the role of earthquake induced axial force in columns of structures, two simple steel MRF frames subjected to a simple harmonic time-history were statically and dynamically analyzed using different types of lateral load patterns; inverted triangular, first mode-base, full modes, uniform, and finally, IDA approach. It was shown that the axial force value induced in the frame columns due to different analysis methods is notably different. Such difference results in different component deformation capacities, thus different structural force-displacement capacity curves. In order to infer such results from structural analysis, three set of steel structures 3, 4, 6, 8, 9, 12, 15 and 16-stories were designed. The nonlinear static (push-over) analysis of the structures was performed using the aforementioned methods. The storey shears versus storey drift ratios of upper, lower and middle stories were depicted for comparison demonstration of non-linear static responses of structures with those of IDA approach. The standard errors of selected frames were

Table 11. Presentation of the used push-over techniques accuracies.

Top story			Middle story			First story			General level			
Uniform	First mode	Triangular	Uniform	First mode	Triangular	Uniform	First mode	Triangular	Uniform	First mode	Triangular	MRF (story)
11.42	9.22	7.89	5.51	2.20	2.13	2.78	2.24	2.16	4.17	2.52	2.28	3
19.60	14.5	14.3	9.17	6.82	6.10	2.65	5.15	4.6	5.20	4.25	4.22	4
27.15	28.2	26.8	15.74	7.79	8.52	6.29	9.22	10.27	8.15	6.44	6.18	6
16.05	12.7	12.3	13.70	7.21	7.51	3.40	8.55	7.93	7.81	11.26	11.49	8
22.80	17.5	13.7	11.67	6.42	6.58	7.81	14.92	14.79	7.04	20.21	21.57	9
28.70	24.2	20.7	8.68	6.24	5.86	2.24	5.55	5.70	4.12	19.54	22.90	12
44.10	49.6	25.1	20.40	18.01	15.70	2.28	5.75	6.57	9.44	16.20	14.56	15
46.96	40.8	28.1	16.94	15.54	15.68	4.48	8.60	9.24	5.58	29.50	31.78	16

Table 12. Performance points (P.P.) of frames.

MRF		Shear force of performance point (PP) (KN)□ □				Roof displacement of performance point (PP) (m)			
		Triangular	First mode	Uniform	Dynamic	Triangular	First mode	Uniform	Dynamic
H/B<1.5	3story	403.1	411.2	459.6	460.6	0.071	0.071	0.069	0.131
	4story	584.5	579.3	637.6	676.0	0.138	0.130	0.123	0.166
	6story	1194.9	1224.9	1421.9	1500.5	0.157	0.153	0.132	0.211
1.5<H/B<3	8story	854.5	854.0	978.5	1010.4	0.254	0.245	0.221	0.308
	9story	789.5	798.5	926.1	1002.4	0.204	0.201	0.177	0.249
	12story	1031.3	1062.0	1263	1299.6	0.349	0.339	0.293	0.455
H/B>3	15story	1117.2	1172.1	1393.8	1623.9	0.358	0.343	0.283	0.500
	16story	1244.5	1283.0	1683.6	1856.0	0.405	0.350	0.335	0.561

calculated. With respect to the limited number of tested structures, we have the following conclusions.

The inverted triangular and first mode-based lateral load distribution method mathematically demonstrates smaller component deformation capacity thus, the weaker structural load-deformation capacity. The same results can be drawn in estimation of demands of structures using different non-linear static analysis approaches. Interestingly, while the demand point in a method is at the first part of the moment-rotation curve of beam-column component, in another method it drops from the end of curve showing somehow the failure of the component. Physically, the latter seems to be meaningless. Additionally, while the beam-column in a method behaves as a displacement control member, it behaves as force control in another approach. In all frames, the estimated demand displacements and base shears obtained from nonlinear static

Table 13. Discussion.

		Discussion
Plastic hinge length	Capacity	In critical columns, the capacity curves obtained from IDA approach look higher than those of conventional pushover methods, while those of the triangular lateral load patterns are smaller. The capacity curves of the triangular and first mode load patterns are in-between.
	Demand	The earthquake induced demands obtained from IDA approach are noticeably smaller than those of the three push-over load patterns in critical columns. However, those of the uniform load patterns are greater than triangular and first mode non-linear responses. The non-linear earthquake induced demands of the first mode load patterns intended to be greater than those of uniform as the height of structures increase. It is notable that in critical columns the deformation demand obtained from nonlinear static analysis, in some examples (8, 12-story frames), drop from capacity bounds while those of IDA approach are within force or displacement control domains and the non-linear responses of others are within displacement control area between these two bound.
Levels	General level	In general level in H/B<1.5 the responses obtained from IDA are between triangular load pattern and uniform one and it converges to uniform load pattern capacity curve with the increasing of H/B ratio and going in nonlinear region.
	First story level	In all span ratios, uniform load pattern is more effective and has the smallest S.E in first level.
	Middle story level	In middle level triangular, uniform and elastic first mode pattern diverge from IDA. in all of patterns the S.E values are considerable with the more S.E in uniform and smallest values in triangular load pattern.
	Top story level	In top level, all load patters lead to poor predictions and have considerable differences with IDA responses, therefore the S.E values in all lateral load patterns are more than acceptable values. In addition, in this level S.E values of pushover methods using uniform load pattern are the largest.
Performance points		In all frames the predicted demand displacements and base shears obtained from nonlinear static approach are lower than nonlinear dynamic analyses, in other words, with comparison between IDA results and other load patterns in performance point the demand displacement of triangular and the demand base shear of uniform closed to IDA.

(push-over)approaches are lower than those of nonlinear dynamic analyses, IDA. The demand displacements obtained from triangular and uniform lateral load pattern methods are close to those of IDA and away from those of first mode-base load pattern. The capacity curves obtained from IDA approaches look higher than those of conventional pushover methods, while those of the uniform lateral load patterns are lower. The capacity curves of the triangular and first mode lateral load patterns are in between.

REFERENCES

Abrahamson NA, Silva WJ (1997). Empirical response spectral attenuation relations for shallow crustal earthquake, Seismol. Res. Lett., 68(1): 94-127.

Antoniou S, Pinho R (2004). Advantage and Limitations of Adaptive and Non-Adaptive Forced-Based Pushover Procedure. J. Earthquake Eng., 8(4): 497-522.

Antoniou S, Pinho R (2004). Development and Verification of Displacement-Based Pushover Procedure. J. Earthquake Eng. 8(5): 643-661.

Atkinson GM, Boore DM (2006). Earthquake ground-motion predictions for eastern North America, Bullet. Seismol. Soc. Am., (96): 2181-2205.

Akkar S, Bommer JJ (2007). Empirical prediction equations for peak ground velocity derived from strong-motion records from Europe and the Middle East. Bullet. Seismol. Soc. Am., (97): 511-532.

Applied Technology Council (1996). Seismic Evaluation and Retrofit of Concrete Building. Report ATC40.

Ambraseys NN, Simpson KA (1996). Perdiction of vertical response spectra in Europe. Earthquake Eng. Struct. Dyn. 25(4): 401-412.

ASCE (2005). Minimum design of loads for buildings and other structures. ASCE/SEI 7-05.

Bender B, Perkins DM (1987). SEISRISK III, A computer program for seismic hazard estimation. US Geological Survey.

Bracci JM, Kunnath SK Reinhorn AM (1997). Seismic performance procedure for seismic evaluation of reinforced concrete structures. J. Struct. Eng., 123(1): 3-10

Campbell KW (1981). Near-source attenuation of peak horizontal acceleration, Bulletin of Seismological Society of Am. 71 (6): 2039-2070.

Chopra AK, Goel RK (2001). A modal pushover analysis procedure to estimate seismic demands for buildings: theory and preliminary evaluation. Report(03):PEER.

Chopra AK, Goel RK (1999). Capacity-demand diagram methods for estimating seismic deformation of inelastic structures: SDF systems. Pacific Earthquake Eng. Research Center. p. 2.

Chopra AK, Goel RK (2000). Evaluation of NSP to estimate seismic deformation: SDF systems. J. Struct. Eng., 126(4): 482-90.

Cornell CA (1968). Engineering seismic risk analysis, Bullet. Seismol. Soc. Am., (58): 1583–1606.

Cornell CA (1971). Probabilistic analysis of damage to structures under seismic loads. John Wiley, 473-493.

Elnashai AS, Papanikolaou KV Lee DH (2010). ZEUS-NL(version 1.8.9), A program for inelastic static and dynamic analysis of structures.

FEMA273 (1997). NEHRP guidelines for the seismic rehabilitation of building. Federal Emergency Management Agency.

FEMA356 (2000). Prestandard and commentary for the seismic rehabilitation of building. Federal Emergency Management Agency.

FEMA440 (2005). Improvement of nonlinear static seismic analysis procedures. Federal Emergency Management Agency.

Fajfar P, Gaspersic P (1996). The N2 method for seismic damage analysis of RC buildings, Earthquake Eng. Struct. Dyn., 25(1): 31-46.

Gardner JK, Knopoff L (1974). Is the sequence of earthquakes in southern California with aftershocks removed, poissonian? Bullet. Seismol. Soc. Am., (64): 1363-1367.

International Building Code IBC (2000). International Code Council.

Joyner WB, Boore DM (1981). Peak horizontal acceleration and velocity from strong-motion records including records from the 1979 Imperial Valley. Bullet. Seismol. Soc. Am., (71): 2011–2038.

Kijko A, Sellovoll MA (1992). Estimation of earthquake hazard parameters from incomplete data files. Part II, Incorporation of magnitude heterogeneity. BSSA, 82(1): 120-134.

Krawinkler H, Seneviratna GDPK (1998). Pros and cons of a pushover analysis of seismic performance evaluation. Eng. Struct. J., (20): 452-464.

Lakshmanan N (2003a). Ductility, energy absorption, and damage modelling of concrete structural elements. Proceed. int. conf. recent trends concr. technol. struct., 1: 69-85.

Lakshmanan N (2005a). Analysis and design of concrete structures. Proceedings of the international conference on recent advances in concrete and construction technology. SRM Institute of Technology.

Lakshmanan N (2006). Seismic evaluation and retrofitting of buildings and structures. ISET J. Technol. 43(1-2): 31-48.

McGuire RK (1995). Probabilistic seismic hazard analysis and design earthquakes: Closing the loop. Bullet. Seismol. Soc. Am., (85): 1275-1284.

McGuire RK (2004). Seismic hazard and risk analysis, Earthquake Eng. Res. Instit., (10): 240.

Naeim F(2001). The seismic design handbook. Mc Graw Hill Pub. Chapter(04).

Papanikolaou KV, Elnashai AS, Juan FP (2005). Limits of applicability of conventional and adaptive pushover analysis for seismic response assessment. Mid-America Earthquake Center. Report, pp. 5-2.

Saiidi M, Sozen MA (1981). Simple nonlinear analysis of RC structures. ASCE. (107): 937-951.

Sadigh K, Chang CY, Egan JA, Makdisi F, Youngs RP (1997). Attenuation relationships for motion shallow earthquakes based on California strong motion data. Seismol. Res. Lett., 68(1): 180-189.

Toro GR, Abrahamson NA, Schneider F (1997). Model of strong ground motions from earthquakes in central and eastern North America: Best estimates and uncertainties, Seismol. Res. Lett., 68(1): 41-57.

Vamvatsikos D, Cornell CA (2005). Seismic Performance, Capacity and Reliability of Structures as Seen Through Incremental Dynamic Analysis. Dep. Civil Environ. Eng., p.151.

Youngs RR, Chiou SJ, Silva WJ, Humphrey JR (1997). Strong ground motion attenuation relationships for subduction zone earthquakes. Seismol. Res. Lett., 68(1): 58-73.